

# Adaptive thermal compensation of test masses in advanced LIGO

**Ryan Lawrence, Michael Zucker, Peter Fritschel, Phil Marfuta  
and David Shoemaker**

Department of Physics and Center for Space Research, Massachusetts Institute of  
Technology, Cambridge, MA 02139

E-mail: ryan@ligo.mit.edu

**Abstract.** As the first generation of laser interferometric gravitational wave detectors near operation, research and development has begun on increasing the instrument's sensitivity while utilizing the existing infrastructure. In the Laser Interferometer Gravitational Wave Observatory (LIGO), significant improvements are being planned for installation in  $\sim 2007$ , increasing strain sensitivity through improved suspensions and test mass substrates, active seismic isolation, and higher input laser power. Even with the highest quality optics available today, however, finite absorption of laser power within transmissive optics, coupled with the tremendous amount of optical power circulating in various parts of the interferometer, result in critical wavefront deformations which would cripple the performance of the instrument. Discussed is a method of active wavefront correction via direct thermal actuation on optical elements of the interferometer. A simple nichrome heating element suspended off the face of an affected optic will, through radiative heating, remove the gross axisymmetric part of the original thermal distortion. A scanning heating laser will then be used to remove any remaining non-axisymmetric wavefront distortion, generated by inhomogeneities in the substrate's absorption, thermal conductivity, etc. A proof-of-principle experiment has been constructed at MIT, selected data of which are presented.

Submitted to: *Class. Quantum Grav.*

PACS numbers: 04.80.Nn, 95.55.Ym, 42.60.Lh, 07.60.Ly

## 1. Introduction

As the first generation of the Laser Interferometer Gravity Wave Observatory (LIGO)<sup>‡</sup> nears operation, planning is underway to further improve the instrument’s phase sensitivity. Around 2007, new active seismic isolation systems, new test masses and suspensions, and more powerful lasers will all be installed in the existing infrastructure, with the goal of increasing the broadband phase sensitivity (hence gravitational wave strain sensitivity) of the instrument by at least a factor of 10. The primary contributor to phase noise at gravitational-wave frequencies above 300 Hz is the Poisson fluctuation in detected laser power, termed “shot noise”. In principle, one can increase the optical power in the interferometer to reduce this effect, but only to the fundamental limit where fluctuating radiation pressure randomly perturbing the test mass momenta (a noise source whose amplitude increases with power) overtakes the shot noise, an effect enforced by the Heisenberg Uncertainty limit for detection of the mirror position.

However, the amount of allowable circulating optical power is limited by the nonzero optical absorption in the substrate and coatings of test masses, typically 0.5 parts per million (ppm) per reflection for coatings and 1 ppm/cm for transmission through fused silica substrates. Absorption of the Gaussian-profiled beam induces a nonuniform temperature increase within the optic. This induces nonuniform optical path length distortions through two mechanisms: (1) thermoelastic expansion of the optic’s surface, and (2) variation of the material’s refractive index with temperature (termed “thermal lensing”). One may approximate that, for a collimated Gaussian beam propagating through a cylindrical optic, the absorption-induced optical path difference between the beam center and  $1/e^{-2}$  intensity radius (termed the “waist radius”  $w$ ) is [1]:

$$\delta s \approx P_{abs} \frac{\beta}{4\pi\kappa} \approx 6 \times 10^{-7} \frac{\text{m}}{\text{W}} \left( \frac{1.38 \frac{\text{W}}{\text{m}^{\circ}\text{K}}}{\kappa} \right) \left( \frac{\beta}{1 \times 10^{-5}/^{\circ}\text{K}} \right) P_{abs} \quad (1)$$

$$\text{where } \beta = \begin{cases} \alpha + \frac{dn}{dT}, & \text{in transmission} \\ \alpha, & \text{on reflection} \end{cases}$$

where  $\kappa$  is the thermal conductivity,  $\alpha$  is the thermal expansion coefficient, and  $\frac{dn}{dT}$  is the derivative of the index of refraction with respect to temperature for the substrate material, and  $P_{abs}$  is the optical power absorbed in the optic (in both the substrate and the coatings). Figure 1 details the expected distortions in an advanced LIGO interferometer.

To enable readout and control of the LIGO interferometer’s mirror positions, a deliberate arm length asymmetry of about 22 cm is introduced to the power recycling cavity (a nearly degenerate cavity consisting of the recycling mirror and the high reflectivity surface of the two arm cavity input couplers), and radio-frequency (RF) sidebands are impressed on the input laser light which resonate in the Michelson cavity and are anti-resonant in the arm cavities [2]. With this in mind, the deleterious effects

<sup>‡</sup> <http://www.ligo.caltech.edu>

of thermal lensing and thermoelastic expansion are seen to be twofold. Firstly, thermal lensing in the beamsplitter, as well as distortions common to both arms (due to the deliberate arm length asymmetry), result in imperfect interference at the antisymmetric port; this results in additional light on the photodetector which contains no information about the instrument’s differential arm length, but contributes shot noise nonetheless. Secondly, thermal lensing in the input test masses can cause the power recycling cavity to become unstable for the RF sidebands.

To calculate the effects thermal distortions have on the circulating optical fields in the instrument we use the Melody§ modal model of the LIGO interferometer [3, 4]. Knowing the fields in the modeled interferometer, we calculate the shot noise limited phase sensitivity as [5]:

$$\Delta\tilde{\phi}(f) = \left( F_{ns} \sqrt{1 + R_{bs} \frac{1 - C}{4 \sin^2(2k_m \delta l)}} \right) \sqrt{\frac{2\hbar\omega}{P_{bs}}} \quad (2)$$

where  $F_{ns}$  is the non-stationary correction factor ( $\sqrt{3/2}$  for the current readout scheme),  $k_m = 2\pi f_m/c$  is the modulation wavenumber for the resonant sidebands,  $R_{bs}$  is the ratio of carrier power to sideband power at the beamsplitter,  $C \equiv (P_{bs} - P_{as})/(P_{bs} + P_{as})$  is the fringe contrast,  $\omega$  is the laser light frequency,  $P_{bs}$  is the carrier power incident on the beamsplitter, and  $P_{as}$  is the total carrier power at the antisymmetric port. Figure 4 shows the carrier power expected at the antisymmetric port, as well as the resulting phase noise, as a function of interferometer input power.

### 1.1. Thermal compensation

Research is underway on techniques of avoiding the problem of power absorption in LIGO optics. Identifying and reducing the source of bulk optical absorption in test mass material is one obvious solution [7]. One may also change the topology of the interferometer to an all-reflective one [6], which exploits the fact that thermal expansion coefficient for fused silica is  $\sim 20\times$  smaller than its  $\frac{dn}{dT}$ . We discuss a method of directly addressing the problem by “thermal compensation”: one may attempt to homogenize the absorption-induced temperature fields by radiatively depositing additional heat on the surface of the optic in a tailored pattern, thus compensating the original distortion. We investigate two methods for thermally compensating distortions in the LIGO interferometer. First, one may arrange radiative heating elements and reflectors to thermally compensate the anticipated beam-induced thermal distortions. This method is expected to work well for distortions whose form can be calculated in advance. More generally, a scanning laser beam with a wavelength which is strongly absorbed by the optic’s substrate can be used to actively tailor the heating pattern to address non-axisymmetric distortions induced by possible optical inhomogeneities and surface impurities. Figure 2 sketches the two modes of thermal compensation we investigate.

§ available at the URL <http://www.phys.ufl.edu/LIGO/LIGO/STAIC/SOFT/>

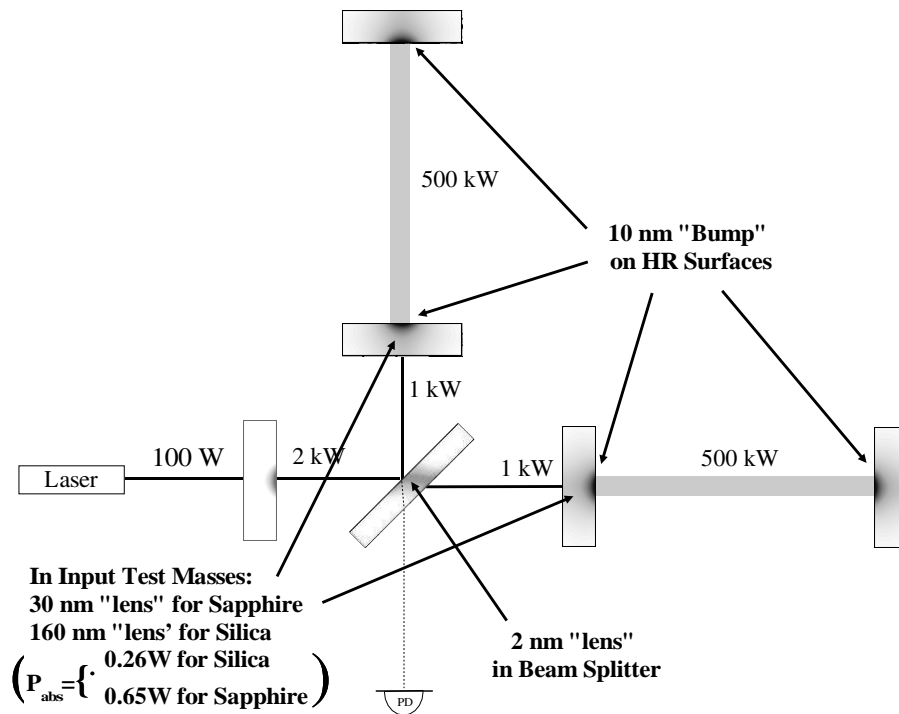


Figure 1. Projected thermal effects in advanced LIGO.

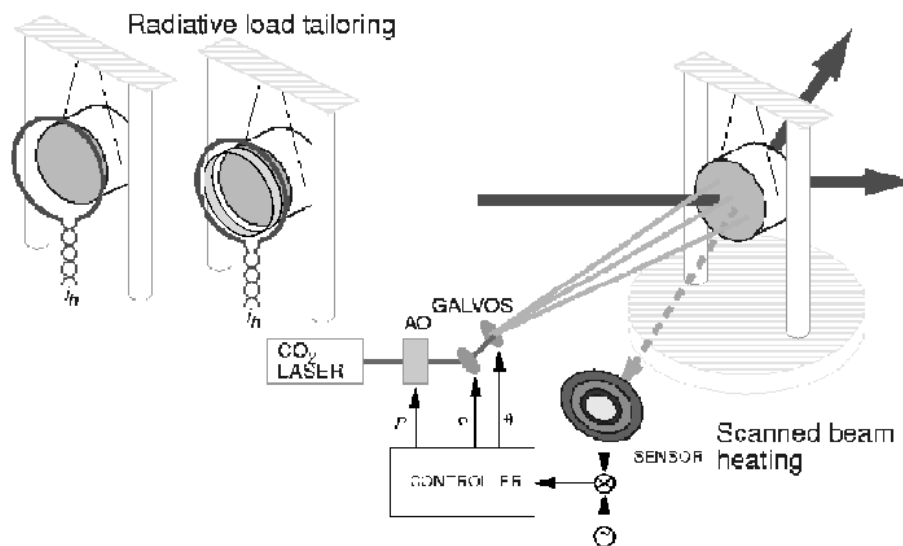


Figure 2. Compensation methods.

To determine the effects of a given heating pattern on the surface of the optic, we have constructed a two dimensional finite element model which, given a one dimensional heating pattern (axisymmetric heating), numerically solves the partial differential equations (PDE's) governing heat transfer, then uses the calculated temperature field to solve the PDE's governing thermoelastic deformations. As a figure of merit for a

given correction, we use the resulting corrected wavefront distortion to calculate the total power scattered out of the incident TEM<sub>00</sub> LIGO beam into higher order spatial modes upon reflection or transmission by the corrected optic. A second practical figure of merit is the maximal temperature increase of the optic, including the heat added by our thermal correction, per Watt of absorbed optical power compensated.

Finally, we note that it is not entirely necessary to directly thermally actuate the optic whose distortions we wish to correct, but may instead impose the correction on a separate, purely transmissive compensation plate placed in the optical chain. Sapphire, the material proposed for the advanced LIGO test masses, has a thermal conductivity  $\sim 30\times$  larger than fused silica as well as a high transmission for wavelengths shorter than  $6\ \mu\text{m}$ : two properties which make sapphire undesirable compared to fused silica for direct thermal actuation. For the remainder of this paper, we discuss the effects of thermal compensation on fused silica optics only.

## 2. Axisymmetric thermal compensation

We first consider a thin heating ring, mounted at a distance  $H$  from the face of the optic and axially centered on the optical axis (symmetry axis) with a radius  $R$  larger than the optic's radius (to prevent interference in the clear aperture)). Inserting the calculated heating pattern into our finite element model to calculate wavefront corrections, and optimizing over  $R$ ,  $H$ , and the ring power  $P_{ring}$ , we find a 100-fold reduction in the power scattered into higher order modes. However, this comes at the cost of a temperature increase of  $375^\circ\text{K}$  per Watt of optical power compensated. The simple ring is thus deemed impractical for realistic thermal compensation.

One clear contributor to the inefficiency of the single heating ring is the fact that some of its radiation falls in the center of the optic, where the beam heating which we are attempting to compensate is concentrated. One method of eliminating this spurious central heating is to include a passive cylindrical shield, with a radius equal to the optic's (thus smaller than the ring's), and a height  $H_s < H$  such that the central portion of the optic is shielded from the ring's radiation. Another contributor to the inefficiency of the single heating ring is the dissipation of heat out the radial surface of the optic. Suspending a low-emissivity aluminum sheath around this surface inhibits radiation exchange with the environment, hence reducing radial temperature gradients.

Again using our finite element model to optimizing over  $R$ ,  $H$ ,  $H_s$ , and  $P_{ring}$ , we find a 1000-fold reduction in TEM<sub>00</sub> scatter is achievable over a broad range of  $R$  and  $H$ , at the cost of a temperature increase in the substrate of  $48^\circ\text{K}$  per watt of optical power compensated. Figure 3 shows an optimized corrected wavefront for the shielded ring actuating an insulated fused silica input test mass of LIGO I dimensions (radius 12.5 cm, height 10 cm, beam waist 3.6 cm).

Inserting the corrected wavefront distortions for an input test mass into the Melody model of the interferometer, we calculate the effects of thermally actuating the test masses on the circulating fields of the interferometer. Calculating the phase noise

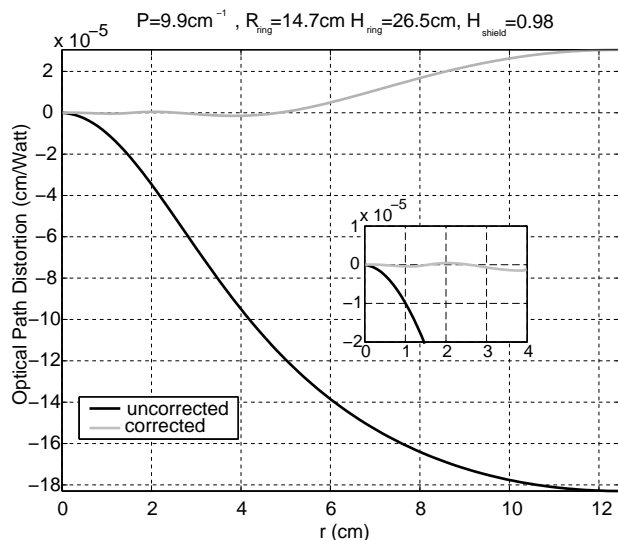


**Figure 3.** Optical path distortion through a fused silica input test mass, per Watt of absorbed optical power.

component, we further optimize to compensate the beamsplitter lens by adjusting the correction amplitude (i.e., the heating ring power) on the test masses. Figure 4 shows the instrument’s performance with the input test masses compensated as detailed in figure 3, with a relative compensation amplitude of 1.00 in the X arm input test mass, 0.95 in the Y arm input test mass.

### 3. Scanning laser thermal compensation

In the case where the material properties of our optics (absorption, thermal conductivity, etc.) are not perfectly homogeneous, additional non-axisymmetric distortions may need to be compensated. We use a well absorbed laser beam, amplitude modulated and scanned over a single face of an actuated optic. By tailoring the power deposited in over a discrete, constant scanning pattern with a scan period small compared to the local thermal time constant  $\tau_l$  ( $\sim w_h^2 \rho c / \kappa$  where  $\rho$  the density,  $c$  the heat capacity,  $\kappa$  the thermal conductivity of the optic, and  $w_h$  the heating beam waist radius), one can compensate a subset of all possible wavefront distortions.

Given a fixed scan pattern of  $N$  points, we wish to find the power which must be deposited at each scan point, represented as a vector  $\vec{P}$  of length  $N$ , to produce a given wavefront distortion  $\vec{d}$ , represented as a vector in some  $M$  dimensional basis spanning a subset of  $\mathbf{L}^2(D)$ , the space of integrable 2D functions over a region  $D$  (defined as a circular aperture of radius  $R$ ). We can calculate (or measure) the  $N \times M$  “actuation matrix”  $\underline{A}$  defined such that:

$$\underline{A} \cdot \vec{P} = \vec{d}.$$

Inverting  $\underline{A}$  (or using the technique of Single Value Decomposition in the case that  $\underline{A}$  is

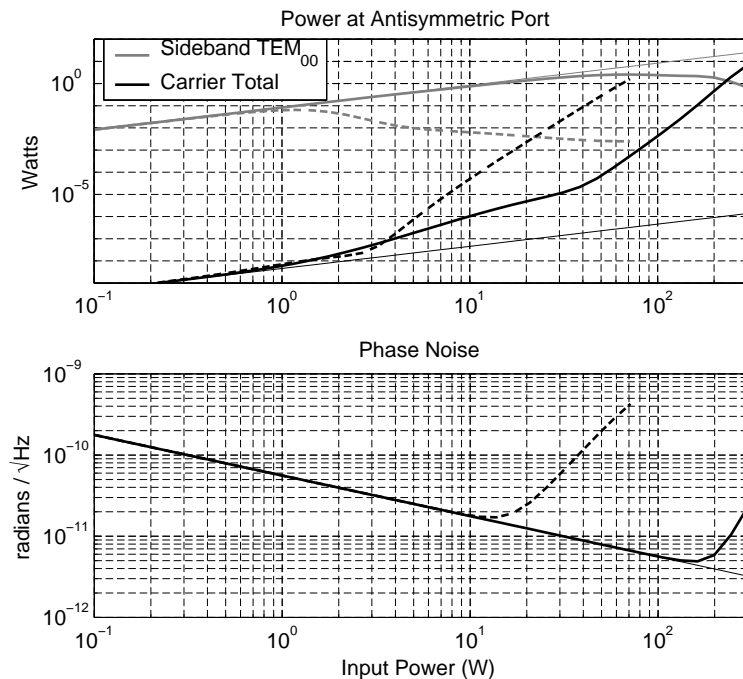


**Figure 4.** Modeled level of output carrier and sideband powers, as well as the detected phase noise (shot noise component) versus optical power at the interferometer input. The broken line is the uncompensated case, the bold line is compensated, and the narrow lines are without any thermal distortions.

not square [8]), we get the  $M \times N$  “response matrix”  $\underline{R} = \underline{A}^{-1}$  such that:

$$\underline{R} \cdot \vec{d} = \vec{P}.$$

Thus, given a wavefront distortion  $\vec{d}$ , we arrive at the power vector required to produce it.

Instead of working in a basis of orthogonal polynomials, it is perhaps simpler to work in the basis of “actuation functions” themselves (the  $k$ th actuation function  $A_k(r, \theta)$ , is the net distortion generated per unit power by the laser actuating on the  $k$ th scan point), which are, in general, not orthogonal in the normal  $\mathbf{L}^2$  sense. As long as each function  $A_k(r, \theta)$  is linearly independent of the previous  $k - 1$  functions, it is possible to construct an orthogonal basis from the  $A_k$  that spans the space of compensatable wavefronts for a given scan pattern (see, for example, [9]). Hence, we may decompose a given wavefront  $\Phi(r, \theta)$  directly into our non-orthogonal basis  $\{A_k\}$  with the standard normalized inner product, i.e.,:

$$d_k = \frac{\int \int A_k(r, \theta) \Phi(r, \theta) r dr d\theta}{\int \int A_k^2(r, \theta) r dr d\theta}$$

and clearly  $P_k = d_k$ .

This result is, in general, not positive for all  $k$ , which is problematic since we cannot actuate on an optic with negative power. The direct way to bypass this is to utilize the

fact that a “deformation” which is constant over the aperture  $D$  is compensatable by simply moving the optic we wish to compensate. Adding an arbitrary constant  $C$  such that  $\Phi + C \geq 0$  over the entire aperture ensures that all the  $P_k$  are  $\geq 0$ . However, to fully span the subspace of compensatable wavefronts, we must be able to generate  $-A_k$  just as well as we can generate  $A_k$ . More generally, we must be able to generate all linear combinations [9]:

$$c_1 A_1 + c_2 A_2 + \dots + c_N A_N.$$

Again utilizing the fact that we do not need to compensate “distortions” which are constant over the aperture  $D$ , an additional (sufficient) condition for our basis of actuation functions to fully span the subspace is that:

$$C = \sum_{n=1}^N A_n(r, \theta)$$

where  $C$  is some constant. The fulfillment of this condition puts a rigorous constraint on the scan patterns we may choose.

#### 4. Thermal compensation experiment at MIT

Figure 5 diagrams the experiment at MIT to experimentally test the basic principles of both axisymmetric and scanning-laser thermal compensation. We use a Shack-Hartmann wavefront sensor to detect changes in optical path when we thermally actuate the test optic through either a scanned CO<sub>2</sub> laser or a shielded heating ring. The optic under test is radially insulated with aluminum foil, and mounted in high vacuum ( $1 \times 10^{-6}$  mBar). The probe source is a fiber pigtailed diode laser ( $\lambda = 635\text{nm}$ ), coupled into a single mode fiber and collimated with a grin lens. The beam is expanded to the size of the optic under test, which is mounted in a high vacuum chamber. The reflected beam from transmission through the optic is sent back through the optical system, where it is diverted with a quarter-waveplate/polarizing beamsplitter and directed into a commercial Shack-Hartmann wavefront sensor. Wavefront slopes relative to the initial “cold” wavefront are resolved over the Shack-Hartmann sensor’s  $32 \times 24$  lenslet grid, and the resulting optical path distortion is reconstructed over the clear aperture.

Initial data taken for the shielded ring actuator shining on a fused silica test optic (5 cm radius, 8 cm depth) can be seen in figure 6, and are in good agreement with theory. However, a decay in the correction magnitude was seen over time, mainly due to re-radiation of the heat shield which was not thermally grounded in an adequate manner.

Initial tests have been completed on the same fused silica test optic for the scanning laser [10], and select data can be seen in figure 7. Here we have used the basis of Zernike polynomials to numerically compute the response matrix, as we have discussed in the first part of section 3. The aperture is 2.5 cm in radius, and the actuating beam has a waist radius 0.5 cm. Our initial calculations disregarded thermal expansion terms in the actuation matrix, as  $\frac{dn}{dT}$  is about  $10\times$  larger than  $\alpha$  in fused silica. The spatial

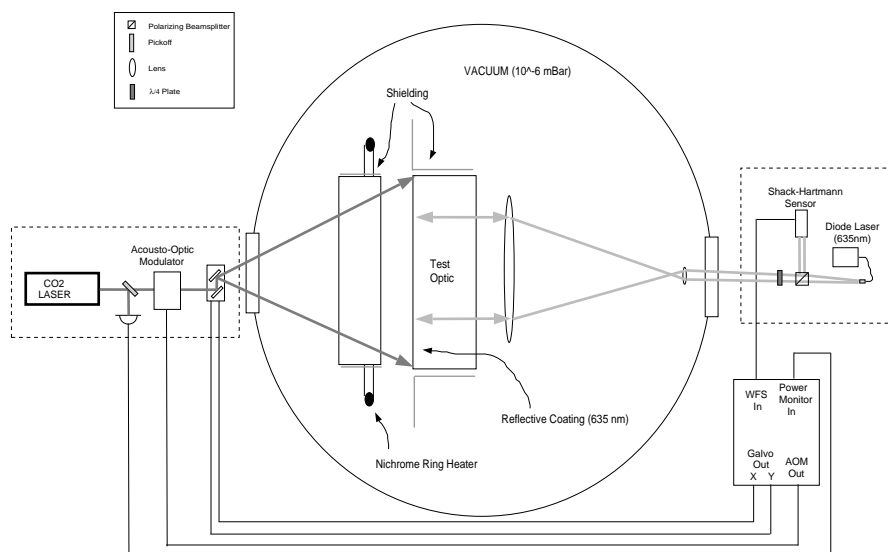


**Figure 5.** Schematic of the experiment.

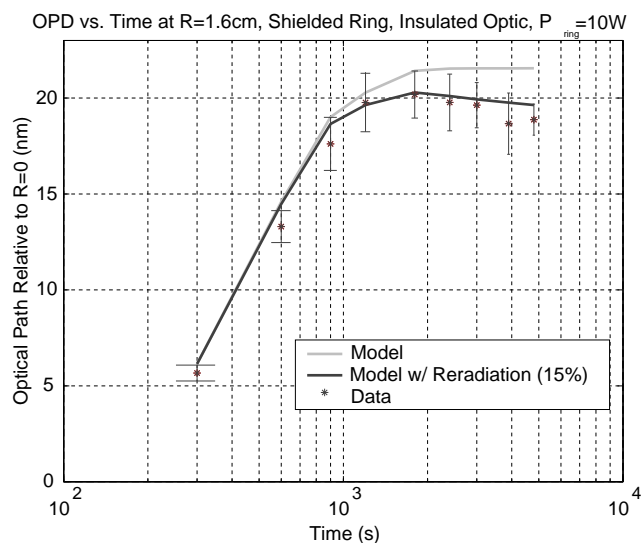


**Figure 6.** Optical path distortion at  $r = 16\text{mm}$  versus time for a shielded ring actuator on a fused silica test optic ( $R = 5\text{cm}$ ,  $H = 8\text{cm}$ ).

frequency of the recreated wavefronts was limited by the beam size in this test, and we could not reproduce Zernike terms higher than  $N = 10$  (i.e.,  $Z_{33}$ ). Also, the net positive amount of power deposited on a single face of the optic caused it to thermoelastically bow, thus giving a persistent curvature term in these data. Since we are working in the regime of small temperature increases, as well as small physical distortions, taking thermal expansion terms into account when calculating the actuation functions will eliminate the persistent curvature.

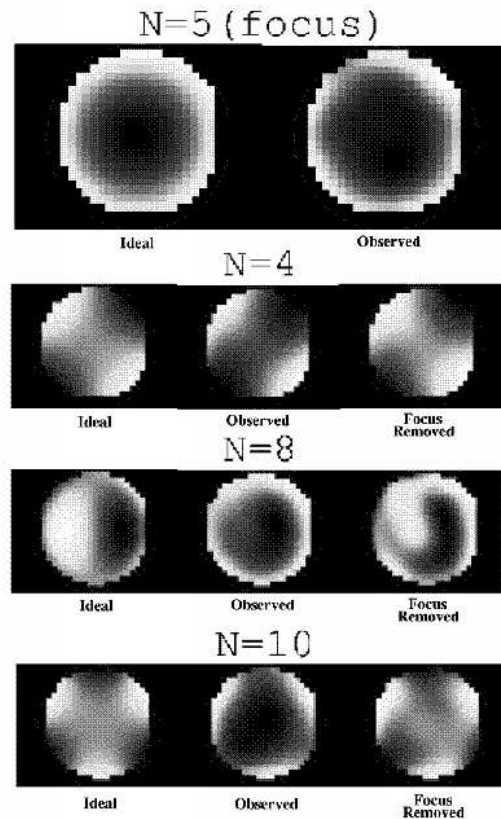


**Figure 7.** Zernike polynomials experimentally replicated by transmission through a fused silica test optic.

## 5. Conclusions

We have discussed the numerical and analytical work done toward solving the problem of thermally compensating the thermal distortions induced in the next generation of LIGO. Using our numerical model to find an optimum correction for a given distortion, we insert the results into a modal model of the entire interferometer and find that a shielded ring heater actuating on the recycling cavity side of the arm cavity input couplers can facilitate the proposed operating power of advanced LIGO with fused silica test masses. In addition, we have begun both analytical and experimental work on developing a scanning laser actuator to compensate any non-axisymmetric wavefront distortions that may be present themselves in the actual advanced LIGO optics.

## Acknowledgments

We thank R. Weiss and P. Schechter for useful discussions and ideas, and are especially grateful to R. Beausoleil for the use of and technical advice regarding Melody. This work was supported by NSF grant PHY-9210038.

## References

- [1] Winkler W, Danzmann K, Rüdiger A, and Shilling R 1991 *Phys. Rev. A* **44** 7022.
- [2] Sigg D, Mavalvala N, Giame J, Fritschel P, and Shormaker D 1998 *Appl. Optics* **37** 5687-5693.
- [3] Beausoleil R and Sigg D 1999 *J. Opt. Soc. Am.* **16** 2990-3002.
- [4] Beausoleil R 2001 *Melody/Matlab: Object-Oriented Model of Gravitational-Wave Interferometers Using Matlab*, LIGO internal document (LIGO document number LIGO-G010301-00-Z).
- [5] Fritschel P, Gonzalez G, Lantz B, Saha P, and Zucker M 1998 *Phys. Rev. Lett.* **80** 3181-3184.
- [6] Beyersdorf P T 2001 *The Polarization Sagnac Interferometer for Gravitational Wave Detection* Ph.D. Thesis, Stanford University (LIGO document number LIGO-P010008-00-Z).
- [7] Alexandrovski A, Route R K, Fejer M M 2001 *Absorption Studies in Sapphire*, LIGO internal document (LIGO document number LIGO-G010152-00-Z).
- [8] Tyson R K 1998 *Principles of Adaptive Optics* (Boston, Ma: Academic Press).
- [9] Riez F and Sz.-Nagy B 1990 *Functional Analysis* (Mineola, NY: Dover Publications) 66-73.
- [10] Marfuta P 2001 *Testing Dynamic Thermal Compensation of Optics for Use in LIGO II* B.Sc. Thesis, Massachusetts Institute of Technology (LIGO document number LIGO-P010011-00-R).